The Astrophysical Journal, 520:714–718, 1999 August 1

DETECTION OF COLLIMATED BIPOLAR OUTFLOWS IN THE PLANETARY NEBULA NGC 6572 SHAPING ITS NEBULAR SHELL

Luis F. Miranda
Instituto de Astrofísica de Andalucía, CSIC, Apartado Correos 3004, E-18080 Granada, Spain; lfm@iaa.es
Roberto Vázquez
Instituto de Astrofísica de Andalucía, CSIC, Apartado Correos 3004, E-18080 Granada, Spain; and Instituto de Astronomía, UNAM, Apartado Postal 877, 22800 Ensenada, B.C., México; vazquez@bufadora.astrosen.unam.mx
Romano L. M. Corradi
Instituto de Astrofísica de Canarias, Vía Láctea s/n, E-38200 La Laguna, Tenerife, Spain; rcorradi@ll.iac.es
Martín A. Guerrero
Instituto de Astrofísica de Canarias, Vía Láctea s/n, E-38200 La Laguna, Tenerife, Spain; and Department of Astronomy, University of Illinois at Urbana-Champaign, 1002 West Green Street, Urbana, IL 61801; mar@astro.uiuc.edu
J. Alberto López
Instituto de Astronomía, UNAM, Apartado Postal 877, 22800 Ensenada, B.C., México; jal@bufadora.astrosen.unam.mx
and
José M. Torrelles
Institut d'Estudis Espacials de Catalunya (IEEC/CSIC), Edifici Nexus, Gran Capità 2-4, E-08034 Barcelona, Spain; and Instituto de Astrofísica de Andalucía, CSIC, Apartado Correos 3004, E-18080 Granada, Spain; torrelles@ieec.fcr.es
Received 1998 November 9; accepted 1999 March 9

ABSTRACT

Highly collimated bipolar outflows have been detected in the planetary nebula NGC 6572 via ground-based optical imagery and high-resolution long-slit spectroscopy. Kinematics and morphology together provide strong evidence of a direct interaction between the collimated outflows and the nebular elliptical shell, creating a double point-symmetric structure. As a consequence of this interaction, the elliptical shell has been broken up, and in this process parts of the shell have been accelerated, while the collimated outflow has been slowed down and/or deflected. These results strengthen the notion that collimated outflows are common in planetary nebulae and may play an important role in shaping the nebular shells. In addition, our kinematic data give a solid confirmation of previous estimates used to derive the distance to this nebula with the parallax expansion method.

Subject headings: ISM: jets and outflows — ISM: kinematics and dynamics — planetary nebulae: individual (NGC 6572)

1. INTRODUCTION

Since its discovery by Struve in 1825 (see Acker et al. 1992), NGC 6572 has been one of the most extensively observed planetary nebulae (PNs), with over 560 references listed in the SIMBAD bibliographic server. Infrared images and radio-continuum maps show an elliptical nebula with bright equatorial regions (Hora et al. 1990; Hajian, Terzian, & Bignell 1995, hereafter HTB; Latter et al. 1995; Kawamura & Masson 1996, hereafter KM). Photometric variability, variability of the nebular emission lines, and dramatic changes of the stellar spectrum are observed in NGC 6572 (Méndez, Manchado, & Herrero 1988; Feibelman, Aller, & Hyung 1992; Arkhipova, Kostyakova, & Noskova 1994); all these indicate a noticeable internal activity. In addition, NGC 6572 represents a particularly interesting case for study because it is one of the few PNs for which the angular expansion has been accurately measured, providing a rare opportunity to apply the parallax expansion method to derive a reliable distance (Liller, Welther, & Liller 1966; HTB; KM; Terzian 1997).

Even though numerous observations of NGC 6572 have been obtained, its internal structure at optical wavelengths remains unknown. Optical images show an elliptical envelope but not internal details (Jewitt, Danielson, & Kupferman 1986; Schwarz, Corradi, & Melnick 1992). High-resolution long-slit optical spectra of NGC 6572 have not been reported so far. This kind of data allows us to study the internal kinematics and to identify the mass ejection processes involved in the formation of the object (e.g., Miranda, Guerrero, & Torrelles 1999). In addition, kinematic information is necessary to obtain the distance by the parallax expansion method.

In this paper we report on narrowband optical images and high-resolution long-slit spectra of NGC 6572, which show details of its internal structure and kinematics. Moreover, the data reveal the presence of collimated bipolar outflows in NGC 6572. Although collimated outflows have already been observed in a number of PNs (e.g., López 1997), in the case of NGC 6572 not only are the collimated outflows detected, but their interaction with the nebular shell is also clearly observed. These findings have important consequences for understanding the formation and shaping of PNs.

2. OBSERVATIONS

Direct images were obtained on 1998 July 9 with the Calar Alto Faint Object Spectrograph (CAFOS) at the 2.2 m telescope at the Calar Alto Observatory.[1] We used nar-

[1] The Calar Alto Observatory is operated by the Max-Planck-Institut für Astronomie (Heidelberg) and the Spanish Comisión Nacional de Astronomía.

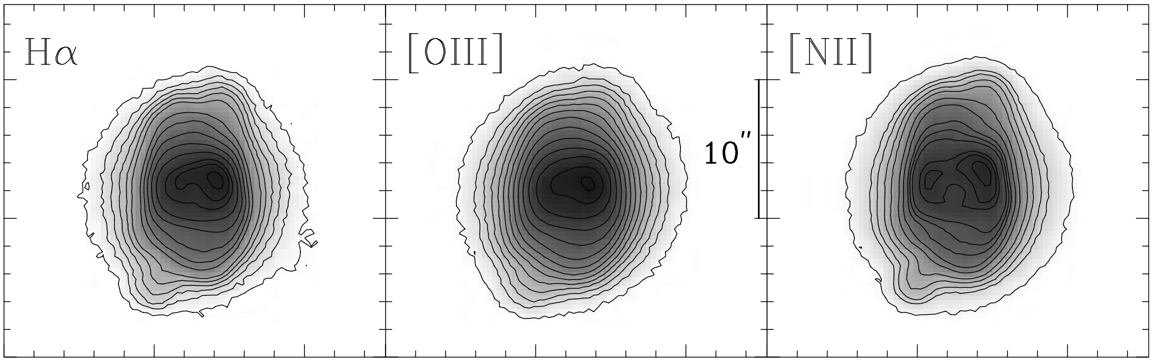

FIG. 1.—Contour and gray-scale Hα, [O III] λ5007, and [N II] λ6583 maps of NGC 6572. North is up, east is to the left.

rowband filters centered in Hα (FWHM 15 Å, exposure time 10 s), [N II] λ6583 (FWHM 19 Å, exposure time 45 s), and [O III] λ5007 (FWHM 25 Å, exposure time 10 s). Spatial resolution is ≃1″.4. Figure 1 presents gray-scale and contour maps of the Hα, [O III], and [N II] images. Figure 2 shows a gray-scale map of the [N II]/[O III] image ratio in which low- and high-excitation regions can be identified.

Long-slit spectra were obtained on 1998 August 1 using IACUB at the Nordic Optical Telescope on Roque de los Muchachos Observatory.[2] The Hα and [N II] λ6583 emission lines were observed at a dispersion of 2.5 Å mm^{-1}. Four spectra were obtained with the slit centered on the object and oriented at position angles (P.A.s) of −18°, 0°, 15°, and 90°, respectively. Exposure time was 900 s for each spectrum. The spectral resolution (FWHM) is ≃8 km s^{-1}, while the spatial resolution is ≃1″.3. Position-velocity (PV) contour maps of the [N II] emission line at the three most relevant P.A.s (−18°, 15°, and 90°) are presented in Figure 3. The PV map at P.A. 0° (not shown here) is very similar to that at P.A. 15°. Radial velocities with respect to the deduced systemic velocity, $V_{\rm LSR} \simeq -10$ km s^{-1}, are indicated in Figure 3.

[2] The IACUB uncrossed echelle spectrograph was built in a collaboration between the IAC and the Queen's University of Belfast. The Nordic Optical Telescope is operated on the Island of La Palma by NOTSA in the Spanish Observatorio del Roque de los Muchachos of the Instituto de Astrofísica de Canarias.

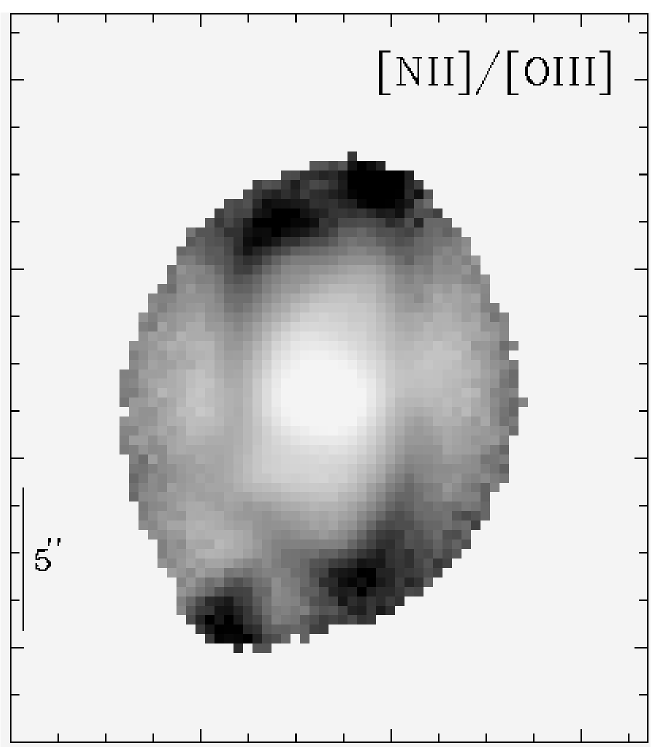

FIG. 2.—Grey-scale [N II]/[O III] image ratio. Black and white regions represent relatively strong [N II] and [O III], respectively. North is up, east to the left.

3. RESULTS AND DISCUSSION

3.1. *Point Symmetry and Collimated Outflows*

The images of NGC 6572 (Fig. 1) reveal two pairs of point-symmetric features in the nebula. One pair is oriented at P.A. −18° and protrudes from the shell. The other pair is observed at P.A. 15° and appears more embedded in the shell. Moreover, the [N II]/[O III] "excitation" map (Fig. 2) shows remarkably well a point-symmetric distribution of four relatively low excitation compact regions, which correspond to the features observed in the images. These features, in particular the P.A. −18° ones, can also be identified in the infrared images of Latter et al. (1995).

The spectra show that the P.A. −18° features are indeed extended along the spatial direction, with sizes of 4″ and 5″ for the northern and southern ones, respectively, and can be traced farther inside the nebula than observed in the images (Fig. 3). An inner and an outer knot are identified in each feature. The inner knots are located at 5″ from the center and present identical but opposite radial velocity (±38 km s^{-1}), which is the largest observed in the [N II] line. The outer knots, corresponding to those observed in the images, show a radial velocity lower than that of the inner knots and exhibit asymmetries in position and radial velocity, as well as different intensities. The [N II] line profile in these features is relatively narrow, with a (mean) FWHM ≃ 17 km s^{-1} (instrumental resolution corrected).

The P.A. 15° system can be identified in the spectrum at P.A. 15°, with compact knots that are not well separated from the global nebular emission. Similar knots are also observed in the spectrum at P.A. 0°, indicating a certain extent in the P.A. 15° system (see also below). These knots show moderate but opposite radial velocities (±7 km s^{-1}; see Fig. 3). The [N II] velocity width in these knots is identical to that quoted above for the P.A. −18° features.

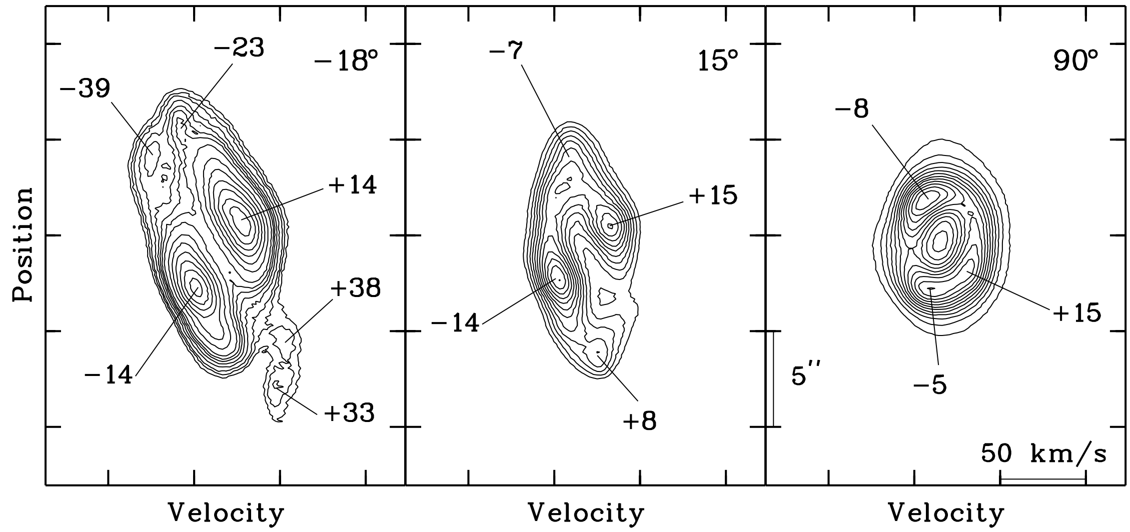

FIG. 3.—Position-velocity contour maps of the [N II] λ6583 emission line as observed at three P.A.s, given in the upper right corner of each panel. Radial velocities (in km s^{-1} with respect to the systemic velocity) are indicated.

[N II]/[O III] values are very similar in the P.A. −18° and P.A. 15° systems (Fig. 2). In the spectra, the [N II] and Hα emissions are of similar intensity, confirming the low excitation suggested by the [N II]/[O III] map. The lowest excitation is observed at the tips of each bipolar system. It is noticeable that at P.A. 15°, the lowest excitation is observed in two compact regions which seem to be the apex of two low-excitation curved arcs, resembling bow-shock–like structures with the concave part facing toward the center of the nebula (Fig. 2). These arcs are relatively extended and can be traced between P.A. ≃ −5° (175°) and ≃30° (215°) and at angular distances from the center of ≃4″.5 and ≃6″, respectively. Within the bow-shock–like structures, the maximum angular distance to the center of ≃6″.6 is observed in the compact regions of lowest excitation.

On the basis of the relatively high radial velocity, small velocity width, and excitation conditions, the P.A. −18° features can be interpreted as highly collimated outflow components. The inner knots at this P.A. represent a bipolar system, while bipolarity is less apparent in the outer knots. Moreover, except for the radial velocity, the P.A. −18° and P.A. 15° bipolar systems share very similar properties, indicating that they might be of similar nature. These results suggest that the two pairs of point-symmetric features are possibly the manifestation of a highly collimated bipolar outflow whose axis has changed its orientation over time or, alternatively, of different collimated outflows in different directions. We note that the radial velocity of the P.A. 15° system is relatively low. This could be due to a small projection angle with respect to the plane of the sky. However, the possibility cannot be ruled out that the intrinsic velocity of the P.A. 15° outflow is relatively low. In fact, collimated bipolar outflows in PNs exhibit a wide range of velocity values (Miranda, Guerrero, & Torrelles 1999 and references therein), and in some cases low velocities have been estimated (e.g., Miranda & Solf 1992). In any case, the observations indicate episodic characteristics for collimated bipolar ejection in NGC 6572. The properties of these outflows are typical of fast, low-ionization emission regions (FLIERS; Balick et al. 1993) and bipolar, rotating, episodic jets (BRETS; López, Vázquez, & Rodríguez 1995).

3.2. *Geometry and Kinematics of the Shell*

The narrowband images also show an ellipsoidal shell with its major axis oriented at P.A. 0° and containing a conspicuous equatorial density enhancement or bright toroidal structure. In the spectra, a "velocity ellipse" is observed at each P.A., although departures from a simple elliptical line shape are apparent.

In the PV maps at P.A.s −18°, 0°, and 15°, the bright toroid produces prominent and well-separated emission maxima, whereas the PV map at P.A. 90° shows a tighter velocity ellipse (Fig. 3). The angular size of the bright toroid, as deduced from the [N II] spectra, is 5″ × 3″. This size has been obtained from the angular separation of the intensity peaks of the emission maxima at P.A. 0° and the maximum angular size of the velocity ellipse at P.A. 90°. Maximum radial velocity (14 km s^{-1}) is observed around P.A. 0°, while at P.A. 90° the maximum angular size of the velocity ellipse is observed essentially at the systemic velocity. These data are compatible with a tilted toroid whose axis is oriented at P.A. 0°. If the toroid is circular, we obtain an inclination angle of 37° for the axis with respect to the plane of the sky and an expansion velocity of 18 km s^{-1} in [N II]. In the Hα spectra (not shown here), well-separated emission maxima due to the toroid are also observed. From Hα we obtain an inclination of 38°, an expansion velocity of 14 km s^{-1}, and a diameter of 3″ for the toroid. The images suggest that the size of the toroid in [O III] is somewhat smaller than in Hα. A (mean) kinematic age of ≃700 yr for this structure is deduced from [N II] and Hα (distance 1.2 kpc, see below). Nevertheless, differences exist between the individual kinematic ages in [N II] (≃790 yr) and Hα (≃610 yr), since in these two species the expansion velocity and radius are not proportional to each other. It is worth noting that the measurement of the radial velocity in long-slit spectra is based on differential measurements, which leads to corresponding small errors. In particular, we estimate an error of ±1 km s^{-1} in the expansion velocity.

The general kinematics of the ellipsoidal shell, as observed in the [N II] emission line, have been analyzed with an ellipsoid model considering that the toroid traces the equatorial plane. In this way, the polar expansion velocity (V_P) is the only additional parameter needed to generate different ellipsoids. In order to illustrate the results, Figure 4 shows the elliptical line shapes expected from two ellipsoids characterized by $V_P = 27$ and 50 km s^{-1}, superposed on the PV map at P.A. 15°. It can be seen that this model is not able to convincingly reproduce the observed PV map. The same was found for other P.A.s and different values of V_P. In particular, whereas the inner ($\simeq 4''$) regions of the nebula are compatible with a relatively slowly expanding ellipsoid (represented by the $V_P = 27$ km s^{-1} velocity ellipse, Fig. 4), the spatio-kinematic properties of the outer regions, corresponding to the P.A. 15° features, suggest a different kinematic regime. These results are noticeable because the global kinematics of elliptical PNs can be described very well using an ellipsoidal geometry (e.g., O'Dell & Ball 1990; Miranda & Solf 1992; see also Frank & Mellema 1994). We have therefore considered whether the kinematics of the shell could have been distorted so that it cannot be described using an ellipsoidal geometry. The data strongly suggest that this is the case. In addition to the results from the model, the PV map at P.A. −18° clearly shows that the shell is open, and a velocity ellipse is difficult to recognize. Moreover, the spectra at P.A.s −18° and 15° are virtually symmetrical with respect to the major nebular axis, and if the shell were an ellipsoid, the PV maps should be virtually identical to each other. However, substantial differences can be appreciated among them. Below (§ 3.4) we will discuss the implications of these results.

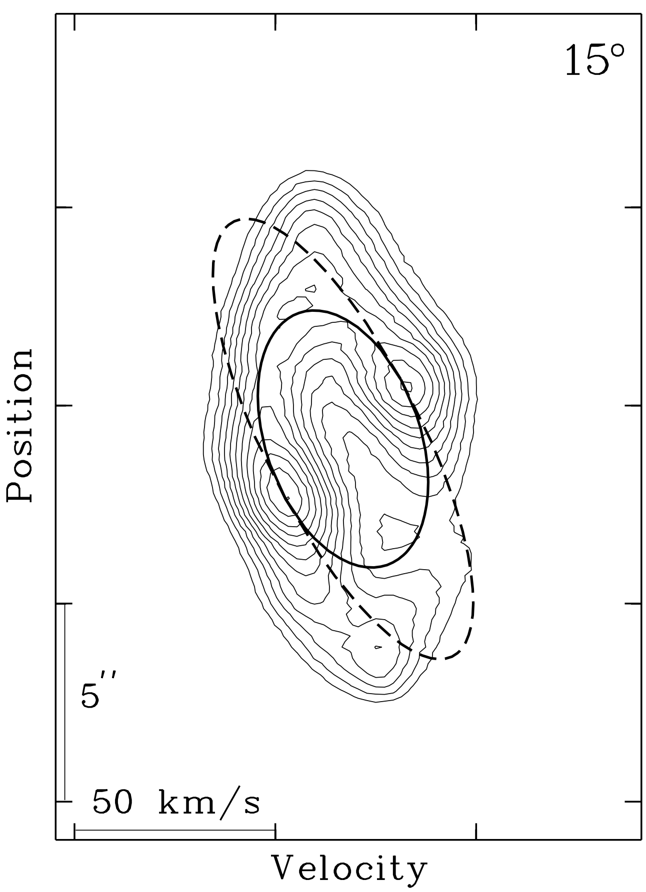

FIG. 4.—Line shapes predicted from a kinematical model of an ellipsoid with polar expansion velocities of 27 km s^{-1} (*solid line*) and 50 km s^{-1} (*dashed line*), superposed on the PV map of the [N II] line at P.A. 15° (see text).

3.3. *The Distance*

Independent measurements by HTB and KM at the 6 cm continuum agree with an angular expansion rate of 2.5 mas yr^{-1} for the toroid. They used an expansion velocity of 14 km s^{-1} to derive a distance of 1.2 kpc. This expansion velocity was obtained from the splitting of published line profiles, corrected for inclination of the nebula, while a large error (± 4 km s^{-1}) was considered to account for the unknown kinematics (see Masson 1989). Our high-resolution long-slit spectra provide new key information about the kinematics and geometry of NGC 6572. We have obtained an inclination angle of 38° for the axis of the toroid, in agreement with the value of 40° deduced by Masson (1989) from modeling the radio continuum emission maps of NGC 6572. In addition, a precise value for the expansion velocity of the toroid in Hα has been deduced. This is important because the Hα and 6 cm continuum emissions trace virtually identical regions, ensuring that both the angular expansion and the expansion velocity refer to the same nebular region (the toroid). Remarkably, our data show that the value used by HTB and KM for the expansion velocity does indeed correspond to the Hα emission, providing a solid support for the distance of 1.2 kpc derived by these authors. Moreover, these results also demonstrate that detailed spatio-kinematic models of PNs based on high-resolution long-slit spectroscopy are necessary to obtain reliable distances by the parallax expansion method, as already pointed out by Hajian & Terzian (1996).

3.4. *Interaction of Nebular Components*

The most important results from the present observations are the detection of collimated bipolar outflows in NGC 6572 and the peculiar kinematics of the shell. The combination of these two results provides conclusive evidence of a strong interaction between the collimated outflow and the shell. This interaction can now be easily recognized at P.A. −18°, where the open-ended shell and the P.A. −18° features are observed. The data also reveal how the collimated outflow has broken up the shell, and how in this process parts of the shell have been accelerated while the collimated outflow has been slowed down and/or has changed its direction. This interpretation explains the peculiar PV map at P.A. −18°. In addition, the different properties of the outer knots could be explained if different physical conditions exist in and/or around each knot, so that the results of the interaction are different in each case. The compact knots at P.A. 15° in the [N II]/[O III] map (Fig. 2) are likely to be tracing the contact points of the collimated outflow with the border of the shell. Evidence for interaction is also indicated by the low-excitation, bow-shock–like structures around these compact knots, suggesting shocked, swept-up material. In this case, our data do not show evidence that the collimated outflow has broken up the shell. This suggests that the collimated outflow–shell interaction at P.A. 15° occurs under different physical conditions from those at P.A. −18°. This could also be related to a possible low velocity of the P.A. 15° system. In any case, a direct relationship between the collimated outflow and the peculiar kinematics of the shell around P.A. 15° is suggested by the observations (Fig. 4; see above).

The new data suggest that three different interacting winds have been involved in the formation of NGC 6572. A first slow wind from the red giant progenitor produces a dense equatorial zone (e.g., Hora et al. 1990). A second fast wind from the central star interacts with the first wind, and the interaction between the fast wind and the anisotropic slow wind results in the formation of an elongated shell (see Zhang & Kwok 1998 and references therein). Finally, a third, collimated bipolar wind (outflow) determines the observed point symmetry and the peculiar kinematics of the shell.

Highly collimated outflows with episodic characteristics and/or changes of direction are observed in an increasing number of PNs, with NGC 6543 and Fg 1 among the most outstanding objects (Miranda & Solf 1992; López, Meaburn, & Palmer 1993; see also López 1997; Corradi et al. 1997; Miranda et al. 1999 and references therein). The detection of this kind of structure in a PN as extensively observed as NGC 6572 provides support for the idea that collimated outflow components may be a common characteristic in the evolution of PNs. Collimated outflows are also invoked to explain point-symmetric structures in PNs (Miranda & Solf 1992; Schwarz 1993; Corradi, Schwarz, Stanghellini 1993; Miranda et al. 1997; Guerrero, Vázquez, & López 1999). *Hubble Space Telescope* images of PNs have shown a large variety of point-symmetric features at or near the border of a shell (Sahai & Trauger 1998; Bobrowski et al. 1998). These elements have been interpreted as a result of collimated outflows interacting with the shell. In NGC 6572 similar point-symmetric structures are apparent in the images. However, here it is the kinematics that provides for the first time the key supporting evidence for that interaction. Monitoring of NGC 6572 at higher spatial resolution is necessary to study the interaction in detail. In addition, it is reasonable to expect that the results of the interaction will depend on the (relative) physical properties of the collimated outflow and shell. Different properties could result in a large variety of collimated and point-symmetric structures, as are in fact observed in PNs. Models and simulations of collimated outflow–shell interaction would be highly valuable to explore the different scenarios suggested by the observations.

We thank an anonymous referee for detailed comments which have improved the presentation and interpretation of the data. We are grateful to the staff of the Calar Alto and Roque de los Muchachos Observatories for helping during the observations. L. F. M., J. M. T., and R. V. are supported partially by Spanish grant PB95-0066. R. V. is in grateful receipt of a graduate scholarship from the AECI (Spain) and complementary support from DGAPA-UNAM (México). M. A. G. is supported partially by Spanish grants PB94-1108 and PB97-1435-C02-01. J. A. L. acknowledges financial support from DGAPA-UNAM through project IN111896. J. M. T. acknowledges the hospitality offered by the Departament de Fisica of the Universitat de les Illes Balears (UIB) and the Instituto Mediterráneo de Estudios Avanzados (CSIC/UIB) (Spain) during the preparation of this paper. This work has been partially supported by the Programa de Cooperación Científica con Iberoamérica.

REFERENCES

Acker, A., Ochsenbein, F., Stenholm, B., Tylenda, R., Marcout, J., & Schohn, C. 1992, Strasbourg-ESO Catalogue of Galactic Planetary Nebulae (Garching: ESO)

Arkhipova, V. P., Kostyakova, E. B., & Noskova, R. I. 1994, Pis'ma Astron. Zh., 20, 122

Balick, B., Ruygers, M., Terzian, Y., & Chengalur, J. N. 1993, ApJ, 411, 778

Bobrowsky, M., Sahu, K. C., Parthasarathy, M., & García-Lario, P. 1998, Nature, 392, 469

Corradi, R. L. M., Guerrero, M. A., Manchado, A., & Mampaso, A. 1997, NewA, 2, 461

Corradi, R. L. M., Schwarz, H. E., & Stanghellini, L. 1993, in IAU Symp. 155, Planetary Nebulae, ed. R. Weinberger & A. Acker (Dordrecht: Kluwer), 216

Feibelman, W. A., Aller, L. H., & Hyung, S. 1992, PASP, 104, 339

Frank, A., & Mellema, G. 1994, ApJ, 430, 800

Guerrero, M. A., Vázquez, R., & López, J. A. 1999, AJ, 117, 967

Hajian, A. R., & Terzian, Y. 1996, PASP, 108, 419

Hajian, A. R., Terzian, Y., & Bignell, C. 1995, AJ, 109, 2600 (HTB)

Hora, J. L., Deutsch, L. K., Hoffmann, W. F., & Fazio, G. G. 1990, ApJ, 353, 549

Jewitt, D. C., Danielson, G. E., & Kupferman, P. N. 1986, ApJ, 302, 727

Kawamura, J., & Masson, C. 1996, ApJ, 461, 282 (KM)

Latter, W. B., Kelly, D. M., Hora, J. L., & Deutsch, L. K. 1995, ApJS, 100, 159

Liller, M. H., Welther, B. L., & Liller, W. 1966, ApJ, 144, 280

López, J. A. 1997, in IAU Symp. 180, Planetary Nebulae, ed. H. J. Habing & H. J. G. L. M. Lamers (Dordrecht: Kluwer) 197

López, J. A.., Meaburn, J., & Palmer, J. W. 1993, ApJ, 415, L135

López, J. A., Vázquez, R., & Rodríguez, L. F. 1995, ApJ, 455, L63

Masson, C. R. 1989, ApJ, 346, 243

Méndez, R. H., Manchado, A., & Herrero, A. 1988, A&A, 207, L5

Miranda, L. F., Guerrero, M. A., & Torrelles, J. M. 1999, AJ, 117, 1421

Miranda, L. F., & Solf, J. 1992, A&A, 260, 397

Miranda, L. F., Vázquez, R., Torrelles, J. M., Eiroa, C., & López, J. A. 1997, MNRAS, 288, 777

O'Dell, C. R., & Ball, M. E. 1990, ApJ, 362, 226

Sahai, R., & Trauger, J. T. 1998, AJ, 116, 1357

Schwarz, H. E. 1993, in 2d ESO/CTIO Workshop, Mass Loss on the AGB and Beyond, ed. H. E. Schwarz (Garching: ESO), 223

Schwarz, H. E., Corradi, R. L. M., & Melnick, J. 1992, A&AS, 96, 23

Terzian, Y. 1997, in IAU Symp. 180, Planetary Nebulae, ed. H. J. Habing & H. J. G. L. M. Lamers (Dordrecht: Kluwer), 29

Zhang, C. Y., & Kwok, S. 1998, ApJS, 117, 341